



FOSSIL CARBON LOAD IN URBAN VEGETATION FOR DEBRECEN, HUNGARY

Tamás Varga^{1*}  • Petra Barnucz¹ • István Major¹ • Zsuzsa Lisztes-Szabó¹ •
A J Timothy Jull^{1,2,3}  • Elemér László¹ • János Péntzes⁴ • Mihály Molnár¹

¹Isotope Climatology and Environmental Research Centre, Institute for Nuclear Research, Hungarian Academy of Sciences (ATOMKI), Debrecen, P.O. Box 51, H-4001, Hungary

²Department of Geosciences, University of Arizona, Tucson, AZ 85721 USA

³University of Arizona AMS Laboratory, Tucson, AZ 85721, USA

⁴Department of Social Geography and Regional Development Planning, University of Debrecen, Debrecen, Hungary

ABSTRACT. Deciduous tree leaf and grass samples were collected in Debrecen, the second largest city in Hungary. The aim of the study was to determine the rate of fossil fuel-derived carbon in urban vegetation. At the locations sampled, C3 and C4 plants close to roads were collected in September 2017. In total, 82 tree and grass leaf samples were gathered at 36 different sampling points all over the city of Debrecen. The radiocarbon (¹⁴C) results of the samples were compared to the local urban background atmospheric ¹⁴CO₂ data to determine the percentage of the fossil fuel-derived carbon in the plants. Based on our results, the average fossil carbon content in the tree and grass leaf samples were 0.9 ± 1.2% and 2.5 ± 2.5%, respectively. The highest fossil carbon content was 9.6 ± 0.6% in a grass and 4.7 ± 0.7% in a tree leaf sample. It appears that the negative fossil carbon content results obtained at urban sampling areas reflect modern carbon emission, where radiocarbon content is higher than the corresponding local background, presumably due to burning of recent wood containing bomb ¹⁴C in the suburbs as well as other possible sources such as litter decomposition or soil CO₂ emission.

KEYWORDS: fossil carbon, grass, leaf, radiocarbon, vegetation.

INTRODUCTION

The ¹⁴C/¹²C ratio in the atmospheric CO₂ is affected by both natural and anthropogenic sources and sinks. The dilution of atmospheric radiocarbon (¹⁴C) may occur by natural fossil emissions such as volcanic gases, but mainly induced by burning of fossil fuels, and this can be estimated using the formula devised by Suess (Suess 1955; Rakowski 2011; Capano et al. 2010; Major et al. 2018). Major anthropogenic fossil CO₂ sources are traditional fossil-fueled power plants, industrial facilities, cement production and road traffic. Conversely, beyond the natural generation by cosmic rays, the enrichment of atmospheric ¹⁴C can be due to contemporary nuclear facilities and nuclear bomb testing, which resulted in the atmospheric ¹⁴C bomb-peak in 1963 (Nydal and Lövsøth 1983). During this period, the natural ¹⁴C level doubled, and increased from 100 percent modern carbon (pMC) to approximately 200 pMC (Buzinny 2006; Graven et al. 2015). The ¹⁴C level has now declined and is close to the pre-bomb level (Levin et al. 2013).

There are many possible methods which are available for the monitoring and estimation of the carbon isotopic ratio of the atmospheric CO₂ (Kuc 1986; Veres et al. 1995; Pawelczyk and Pazdur 2004; Molnár et al. 2007). The most sophisticated way of long-term monitoring is instrumental sampling, where a representative sample can be collected for a specific period of time, using calibrated electronic devices and high purity chemicals. On the other hand, plants can also collect the CO₂ from the air by photosynthesis. Thanks to this biochemical process, we can conduct cost-effective observations over a wide area during the growing season of plants (Levin et al. 1985; Alessio et al. 2002; Quarta et al. 2007; Janovics et al. 2013; Xi et al. 2013; Zhou et al. 2014). CO₂ fixation by photosynthesis provides a way to estimate the proportion of CO₂ from magmatic activity (Shore and Cook 1995; Cook et al. 2001), natural and urban CO₂ emissions (Baydoun et al. 2015), as well as traffic-derived fossil CO₂ emissions (Druffel and Griffin 1995; Levin and Hesshaimer 2000; Varga et al. 2018). Deciduous plants are primarily used for the biomonitoring of ¹⁴C, because the vegetation

*Corresponding author. Email: varga.tamas@atomki.mta.hu.

period of these plants is better defined than the growing season of evergreen species, where the CO₂ collection and storage cannot easily be determined. Using ¹⁴C measurements, numerous studies have investigated the fossil carbon load of rural and urban areas to determine the local Suess effect at local to regional scales. These studies generally used deciduous plant leaves, specifically *Ginkgo biloba* L., *Zea mays* L., *Agropyron repens* (L.) Gould, *Ficus sp.*, *Setaria viridis* (L.) P. Beauv. samples and past studies have shown a low but detectable ¹⁴C dilution close to densely populated areas (Hsueh et al. 2007; Riley et al. 2008; Zhou et al. 2014; Park et al. 2015; Ndeye et al. 2017).

The aim of our study was to determine the Suess effect on the scale of a medium-sized European city (Debrecen, Hungary) and determine the rate of fossil fuel-derived carbon in the vegetation collected in urban areas of different characteristics, such as the downtown, suburbs and a local forested background area. This study mainly focuses on roadsides and crossroads to estimate the traffic-derived carbon component in the vegetation. Plant samples were investigated in many aspects in Debrecen already (Simon et al. 2014; Molnár et al. 2018), but not for ¹⁴C, although the atmospheric CO₂ is continuously monitored at one sampling point in Debrecen since 2008 (Molnár et al. 2010a, Molnár et al. 2010b).

METHODS

Sampling Sites and Plant Samples

Debrecen is the second largest city of Hungary with approximately 200,000 inhabitants. The city is the cultural, industrial, educational center of Hajdú-Bihar county in the Hungarian Northern Great Plain region and is located close the M3-M35 motorway. For this reason, both local and transit traffic are high thus a high fossil carbon load can be expected. During our sampling campaign, in total, 69 tree (woody plant species) and grass (herbaceous species, with exception of three species belonging to family Poaceae) leaf sample pairs at 35 different sampling points were collected throughout the city (Table 1, Figure 1) in order to examine the fossil carbon load in the different districts. Most of the sampled herbaceous species are therophyte. A few taxa are perennial, however, their buds are protected during the unfavorable seasons under a thin soil layer (hemicrypto-geophyte life form) in temperate climate (*Convolvulus arvensis*, *Cynodon dactylon*, *Lolium perenne*, *Poa angustifolia*) (Király 2009). Thus, the leaves of these herbaceous species are not evergreen. The samples were collected as close to the nearest road as possible, the grass samples were picked off at ground level (typically at 0–1-m distance from the edge of the roads) and the tree leaf samples at head height (~180 cm) typically at 0–2-m horizontal distance from the edge of the roads. A minimum 3 pieces of tree and grass leaves were collected at each sampling point. Plant species were identified based on Király (2009). For comparison, we classified the different types of areas inside and around the city as follows: 1: crossroad in suburb; 2: edge of downtown; 3: busy crossroad; 4: botanical garden; 5: forested area in suburb; 6: downtown; 7: suburb; 8: Great Forest Debrecen.

In addition, 13 samples were collected close to each other in the courtyard of the Hertelendi Laboratory (Table 2) within a 50-m circle around a ¹⁴CO₂ atmospheric monitoring station (47.5427N, 21.6237E, 3 m a.g.l), where the local urban atmospheric CO₂ has been sampled since 2008 (Molnár et al. 2010a). This backyard is a minimum of 50 m away from busy roads and intensive industrial activity (Molnár et al. 2010b; Major et al. 2015). In this way, it is possible to compare the ¹⁴C signals in plants during the vegetation period (March–September) to each other and to the local atmospheric ¹⁴CO₂ data taken as background. For a more

Table 1 Sampled plant species and location of sampling in the city.*

Nr. (#)	Latitude	Longitude	Grass species (with photosynthetic pathway)	Species of tree (with photosynthetic pathway)
1	21.6118°	47.5189°	<i>Lolium perenne</i> L. (C3)	<i>Celtis occidentalis</i> L. (C3)
2	21.6196°	47.5234°	<i>Hordeum murinum</i> L. (C3)	<i>Celtis occidentalis</i> L. (C3)
3	21.6124°	47.5296°	<i>Lolium perenne</i> L. (C3)	<i>Sophora japonica</i> L. (C3)
4	21.6031°	47.5285°	<i>Setaria pumila</i> (Poir.) Schult. (C4)	<i>Celtis occidentalis</i> L. (C3)
5	21.6122°	47.5344°	<i>Cynodon dactylon</i> (L.) Pers. (C4)	<i>Quercus robur</i> L. (C3)
6	21.6045°	47.5347°	<i>Convolvulus arvensis</i> L. (C3)	<i>Celtis occidentalis</i> L. (C3)
7	21.6165°	47.5341°	<i>Polygonum aviculare</i> L. (C3)	<i>Lycium barbarum</i> L. (C3)
8	21.6097°	47.5418°	<i>Cynodon dactylon</i> (L.) Pers. (C4)	<i>Celtis occidentalis</i> L. (C3)
9	21.6011°	47.5422°	<i>Setaria pumila</i> (Poir.) Schult. (C4)	<i>Acer saccharinum</i> L. (C3)
10	21.6096°	47.5475°	<i>Setaria pumila</i> (Poir.) Schult. (C4)	<i>Tilia platyphyllos</i> Scop. (C3)
11	21.6069°	47.5559°	<i>Poa annua</i> L. (C3)	<i>Prunus domestica</i> L. (C3)
12	21.6216°	47.5575°	<i>Setaria pumila</i> (Poir.) Schult. (C4)	<i>Quercus robur</i> L. (C3)
13	21.6216°	47.5514°	<i>Lolium perenne</i> L. (C3)	<i>Celtis occidentalis</i> L. (C3)
14	21.6287°	47.5491°	<i>Setaria pumila</i> (Poir.) Schult. (C4)	<i>Platanus x hybrida</i> Brot. (C3)
15	21.6380°	47.5551°	<i>Poa angustifolia</i> L. (C3)	<i>Quercus robur</i> L. (C3)
16	21.6412°	47.5486°	<i>Setaria pumila</i> (Poir.) Schult. (C4)	<i>Celtis occidentalis</i> L. (C3)
17	21.6492°	47.5531°	<i>Cynodon dactylon</i> (L.) Pers. (C4)	<i>Juglans nigra</i> L. (C3)
18	21.6264°	47.5265°	<i>Setaria pumila</i> (Poir.) Schult. (C4)	<i>Acer platanoides</i> L. (C3)
19	21.6320°	47.5273°	<i>Polygonum aviculare</i> L. (C3)	<i>Sophora japonica</i> L. (C3)
20	21.6326°	47.5251°	<i>Lolium perenne</i> L. (C3)	<i>Celtis occidentalis</i> L. (C3)
21	21.6377°	47.5267°	<i>Lolium perenne</i> L. (C3)	<i>Celtis occidentalis</i> L. (C3)
22	21.6465°	47.5231°	<i>Cynodon dactylon</i> (L.) Pers. (C4)	<i>Ailanthus altissima</i> (Mill.) Swingle (C3)
23	21.6459°	47.5292°	<i>Lolium perenne</i> L. (C3)	<i>Sophora japonica</i> L. (C3)
24	21.6392°	47.5299°	<i>Portulaca oleracea</i> L. (C4-CAM)	<i>Sophora japonica</i> L. (C3)
25	21.6381°	47.5377°	<i>Lolium perenne</i> L. (C3)	<i>Sophora japonica</i> L. (C3)
26	21.6425°	47.5436°	<i>Setaria pumila</i> (Poir.) Schult. (C4)	<i>Tilia tomentosa</i> Moench. (C3)
27	21.6251°	47.5417°	<i>Lolium perenne</i> L. (C3)	<i>Celtis occidentalis</i> L. (C3)
28	21.6296°	47.5153°	<i>Setaria pumila</i> (Poir.) Schult. (C4)	<i>Populus nigra</i> L. (C3)
29	21.6299°	47.5329°	<i>Cynodon dactylon</i> (L.) Pers. (C4)	<i>Pyrus communis</i> L. (C3)
30	21.6257°	47.5346°	<i>Setaria pumila</i> (Poir.) Schult. (C4)	<i>Ulmus pumila</i> L. (C3)
31	21.6210°	47.5345°	<i>Convolvulus arvensis</i> L. (C3)	<i>Fraxinus ornus</i> L. (C3)
32	21.6255°	47.5289°	<i>Hordeum murinum</i> L. (C3)	<i>Tilia cordata</i> Mill. (C3)
33	21.6489°	47.5456°	<i>Hordeum murinum</i> L. (C3)	<i>Tilia x euchlora</i> K. Koch. (C3)
34	21.6230°	47.5759°	<i>Anthriscus cerefolium</i> (L.) Hoffm. (C3)	<i>Acer pseudoplatanus</i> L. (C3)
35	21.6230°	47.5759°	<i>Hordeum murinum</i> L. (C3)	—

*The sampling points are shown in Figure 1.

Table 2 Sampled plant species and location of sampling in the courtyard of HEKAL Laboratory.

Sample code	Latitude	Longitude	Grass species (photosynthetic pathway)	Tree species (with photosynthetic pathway)
A	21.6236	47.5427	<i>Festuca heterophylla</i> Lam. (C3)	<i>Corylus avellana</i> L. (C3)
B	21.6237	47.5426	<i>Elymus repens</i> (L.) Gould. (C3)	—
C	21.6237	47.5426	—	<i>Acer negundo</i> L. (C3)
D	21.6237	47.5427	<i>Poa annua</i> L. (C3)	—
E	21.6237	47.5426	<i>Poa annua</i> L. (C3)	<i>Ptelea trifoliata</i> L. (C3)
F	21.6235	47.5427	<i>Festuca heterophylla</i> Lam. (C3)	<i>Picea pungens</i> Engelm. (C3)*
G	21.6235	47.5429	<i>Digitaria sanguinalis</i> (L.) Scop. (C4)	<i>Picea pungens</i> Engelm. (C3)*
H	21.6235	47.5430	<i>Poa annua</i> L. (C3)	<i>Picea pungens</i> Engelm. (C3)*

*Evergreen samples.

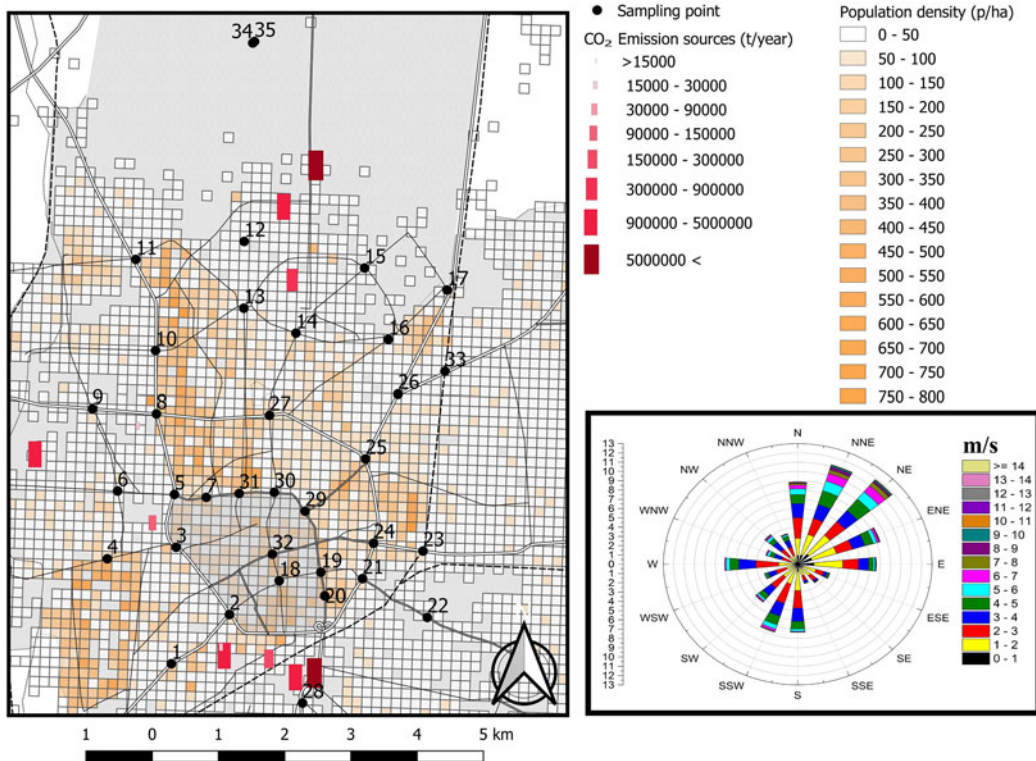


Figure 1 Location of sampling points with the population density, CO₂ emission sources and wind rose of Debrecen during the studied growing season (March–September 2017).

Table 3 Monthly average atmospheric CO₂ ¹⁴C data at Debrecen city and the rural (Hegyhátsál) monitoring stations in the growing season of 2017.

Month (2017)	Hegyhátsál pMC ($\pm 1\sigma$)	Debrecen pMC ($\pm 1\sigma$)	Fossil carbon ratio in Debrecen (%) (rel. HHS)
March	101.1 \pm 0.3	100.5 \pm 0.2	0.6 \pm 0.4
April	100.6 \pm 0.3	100.7 \pm 0.2	-0.1 \pm 0.4
May	101.3 \pm 0.3	101.2 \pm 0.2	-0.1 \pm 0.4
June	101.7 \pm 0.3	101.4 \pm 0.2	0.3 \pm 0.4
July	101.6 \pm 0.3	100.9 \pm 0.2	0.6 \pm 0.4
August	102.0 \pm 0.3	101.4 \pm 0.2	0.6 \pm 0.4
September	102.0 \pm 0.3	101.3 \pm 0.2	0.7 \pm 0.4
Average ($\pm 1\sigma$)	101.5 \pm 0.3	101.1 \pm 0.2	0.4 \pm 0.4

complete description of the sampling area, wind speed and direction data were also collected at an agrometeorological station, 7 km NW of downtown Debrecen.

Sample Preparation and Measurement

The plant-derived samples were kept frozen until preparation. Before sample preparation, the leaves were cut into small pieces and homogenized. The standard Acid-Base-Acid sample preparation method (Southon and Magana 2010) was used for purification of the plant material, then the samples were dried in heating block at 50°C. The purified and dried samples were combusted in sealed tubes at 550°C for 12 hr, using MnO₂ as an oxidant (Janovics et al. 2018) to convert carbon in the organic material to CO₂. The generated CO₂ gas was extracted and purified from other contaminants and H₂O in a dedicated vacuum line. The pure CO₂ gas was subsequently transferred into glass tubes (with Zn, TiH catalysts and iron powder) sealed by flame and converted to graphite following the sealed tube graphitisation method (Rinyu et al. 2013). Finally, the graphite samples were pressed in to aluminium targets for the EnvironMicadas AMS measurements to determine the carbon isotopic composition (Molnár et al. 2013). For data evaluation, “Bats” data reduction software was used (Wacker et al. 2010). For the data evaluation and calculations, percent Modern Carbon (pMC) unit was used (Stenström et al. 2011). The fossil carbon ratio of different samples was determined by the following equation (after Quarta et al. 2007):

$$\text{Fossil carbon ratio (\%)} = \left(\frac{R_B - R_S}{R_B} \right) \times 100 = \left(1 - \frac{pMC_S}{pMC_B} \right) \times 100 \quad (1)$$

Where R_B is the ¹⁴C/¹²C ratio of (local urban) background sample (atmospheric CO₂ from March to September), R_S is the ¹⁴C/¹²C ratio of the plant sample and consequently: pMC_B is the percent Modern Carbon of local urban background sample (atmospheric CO₂ from March to September), pMC_S is the percent Modern Carbon of the plant sample.

RESULTS AND DISCUSSION

Background Atmospheric ¹⁴CO₂ Results in the City

Our urban atmospheric ¹⁴C data in Debrecen shows quite good agreement with that of Hegyhátsál (10 m sampling elevation) regional background station in Western Hungary (46.95N, 16.65E, 248 m a.s.l.) (Table 3). At the Hegyhátsál station, only a slightly diluted

^{14}C ratio can be observed in the growing season, relative to that continental background stations such as Jungfraujoch or Schauinsland (Levin et al. 1985; Major et al. 2018). Consequently, the local atmospheric ^{14}C sampling station in Debrecen (the courtyard of HEKAL) represents an adequate base level to determine the relative local fossil carbon load at the 35 different sampling points in the city.

Urban Vegetation Results

The relative fossil carbon content (%) was calculated from the measured pMC data of the local atmospheric CO_2 background during the growing season (March–September) and urban vegetation (Table 4). The fossil carbon content for all the samples show diverse results with a wide range from -1.9% to 9.6% . It is a narrower range in the case of tree leaves alone (from -1.2% to 4.7%) around a relatively low average fossil carbon load ($0.9 \pm 1.2\%$, $n = 35$). However in grass samples, the average fossil carbon content is $2.5 \pm 2.5\%$ ($n = 35$) ranging from -1.9% to 9.6% (Figure 3). Examining the sample pairs, there is a correlation between the tree leaf and grass leaf sample pairs (Figure 3) regarding their observed fossil carbon ratio, that can be used to confirm the identification of potentially fossil-loaded area. The results obtained of *Celtis occidentalis* (C3 Tree), *Setaria pumila* (C4 Grass) and *Lolium perenne* (C3 Grass) plants show that the fossil-fuel derived carbon is not affected by different photosynthesis routes but the sample location relative to the road and local emission sources (Figures 2 and 3, Table 4).

Removing some outliers, particularly the samples Nr. 12 and 28, the correlation between the sample pairs is relatively strong ($R^2 = 0.4403$, with the outliers the $R^2 = 0.1653$), and suggest that the tree leaves have just about 25% of fossil carbon content compared to their corresponding grass sample pairs. This shows how rapidly the traffic induced CO_2 emission can be diluted as a function of distance from the road. A simple explanation can be that the specimens of grass species grows closer to the roads, and therefore to vehicle exhaust (Figure 3 and Table 4). Since the trees are situated further from the roads, there is enough time for the fossil CO_2 to mix with ambient CO_2 . The relatively rapid mixing and dilution of traffic-derived CO_2 are clearly demonstrated by the results from the courtyard of our institute (Table 5). This area is located inside the city but the sampling points are at least 50 m from busy roads and have generally lower fossil carbon ratios relative to atmospheric CO_2 (average for grasses: $0.6 \pm 0.9\%$ ($n = 6$), for trees: $-0.5 \pm 0.6\%$ ($n = 6$)). These data show that the samples from the yard are in a good agreement with the local atmospheric CO_2 ^{14}C content, that is, the local vegetation can adequately represent the atmospheric carbon isotopic composition of local atmospheric CO_2 .

As discussed above, the fossil carbon content is within a narrow range (from $-1.9 \pm 0.6\%$ to $9.6 \pm 0.7\%$), but sometimes it can be a negative value. A negative fossil carbon load relative to the local background can be explained by biomass and wood burning as carbon sources, which have been affected by the elevated ^{14}C level of the last five decades. Due to the bomb ^{14}C , the biomass that has grown since the 1950s, has slightly higher specific ^{14}C activity than the modern atmospheric CO_2 of the respective years. This effect has already been observed and described in other studies dealing with ^{14}C measurements of carbonaceous aerosols (Heal et al. 2011; Major et al. 2015). In the case of sampling points no. 1 and 33 in the suburbs, where the wood burning is a factor, the results show $-1.9 \pm 0.6\%$ and $-1.4 \pm 0.7\%$ in grass leaves and $-0.5 \pm 0.6\%$ and $-0.8 \pm 0.7\%$ fossil carbon content in tree leaves (Figure 1 and Table 4). This may be amplified by the soil respiration

Table 4 ^{14}C results and calculated fossil carbon ratio in the grass and leaf samples studied.

Location Nr (#)	Grass pMC ($\pm 1s$)	Tree leaf pMC ($\pm 1s$)	Grass Fossil C ratio (%)	Tree leaf Fossil C ratio (%)
<i>Crossroad in suburb</i>				
1	103.0 \pm 0.5	101.6 \pm 0.4	-1.9 \pm 0.6	-0.5 \pm 0.6
6	99.2 \pm 0.4	100.4 \pm 0.4	1.9 \pm 0.6	0.6 \pm 0.6
Average	101.1 \pm 2.7	101.0 \pm 0.8	0.0 \pm 2.7	0.1 \pm 0.7
<i>Edge of downtown</i>				
2	99.7 \pm 0.4	99.9 \pm 0.4	1.4 \pm 0.6	1.2 \pm 0.6
3	96.5 \pm 0.4	99.7 \pm 0.4	4.8 \pm 0.6	1.4 \pm 0.6
4	96.2 \pm 0.4	98.8 \pm 0.5	5.0 \pm 0.7	2.3 \pm 0.6
5	92.3 \pm 0.4	99.5 \pm 0.4	9.6 \pm 0.7	1.6 \pm 0.6
7	97.7 \pm 0.4	99.3 \pm 0.4	3.4 \pm 0.6	1.7 \pm 0.6
20	97.7 \pm 0.4	100.3 \pm 0.4	3.4 \pm 0.6	0.7 \pm 0.6
21	97.9 \pm 0.4	99.9 \pm 0.4	3.2 \pm 0.6	1.1 \pm 0.6
29	98.7 \pm 0.5	99.8 \pm 0.5	2.4 \pm 0.7	1.3 \pm 0.7
30	98.9 \pm 0.5	99.4 \pm 0.5	2.1 \pm 0.7	1.7 \pm 0.7
31	98.0 \pm 0.5	100.8 \pm 0.4	3.1 \pm 0.7	0.3 \pm 0.6
Average	97.7 \pm 2.1	99.7 \pm 0.5	3.8 \pm 2.3	1.3 \pm 0.5
<i>Busy crossroad</i>				
8	98.6 \pm 0.5	99.1 \pm 0.5	2.5 \pm 0.6	1.9 \pm 0.6
9	98.6 \pm 0.4	99.3 \pm 0.4	2.5 \pm 0.6	1.8 \pm 0.6
10	94.5 \pm 0.3	100.1 \pm 0.3	6.9 \pm 0.5	0.9 \pm 0.5
11	95.1 \pm 0.3	98.5 \pm 0.3	6.2 \pm 0.5	2.6 \pm 0.5
13	100.4 \pm 0.3	101.0 \pm 0.3	0.7 \pm 0.5	0.1 \pm 0.5
22	97.2 \pm 0.4	100.3 \pm 0.4	3.9 \pm 0.6	0.8 \pm 0.6
24	94.8 \pm 0.4	99.3 \pm 0.4	6.6 \pm 0.6	1.8 \pm 0.6
25	99.5 \pm 0.5	99.8 \pm 0.4	1.6 \pm 0.6	1.2 \pm 0.6
26	99.7 \pm 0.5	100.9 \pm 0.5	1.3 \pm 0.6	0.2 \pm 0.6
27	95.0 \pm 0.5	100.1 \pm 0.5	6.3 \pm 0.7	0.9 \pm 0.6
28	98.4 \pm 0.5	96.5 \pm 0.5	2.7 \pm 0.6	4.7 \pm 0.7
Average	97.4 \pm 2.2	99.6 \pm 1.3	3.8 \pm 2.4	1.5 \pm 1.3
<i>Botanical garden</i>				
12	101.5 \pm 0.3	98.1 \pm 0.3	-0.4 \pm 0.5	3.0 \pm 0.5
<i>Forested area in suburb</i>				
14	97.9 \pm 0.4	101.5 \pm 0.5	3.2 \pm 0.6	-0.4 \pm 0.6
15	100.2 \pm 0.3	102.3 \pm 0.3	0.8 \pm 0.5	-1.2 \pm 0.5
16	100.5 \pm 0.4	101.4 \pm 0.5	0.6 \pm 0.6	-0.3 \pm 0.6
17	100.9 \pm 0.3	102.0 \pm 0.3	0.1 \pm 0.5	-0.9 \pm 0.5
Average	99.9 \pm 1.3	101.8 \pm 0.4	1.2 \pm 1.4	-0.7 \pm 0.4
<i>Downtown</i>				
18	101.3 \pm 0.3	101.5 \pm 0.3	-0.2 \pm 0.5	-0.4 \pm 0.5
19	99.5 \pm 0.5	99.9 \pm 0.5	1.6 \pm 0.6	1.1 \pm 0.6
32	99.4 \pm 0.5	100.6 \pm 0.5	1.6 \pm 0.7	0.4 \pm 0.7
Average	100.1 \pm 1.1	100.7 \pm 0.8	1.0 \pm 1.0	0.4 \pm 0.8
<i>Suburb</i>				
23	101.3 \pm 0.4	101.3 \pm 0.4	-0.2 \pm 0.6	-0.3 \pm 0.6
33	102.5 \pm 0.5	101.9 \pm 0.5	-1.4 \pm 0.7	-0.8 \pm 0.6
Average	101.9 \pm 0.8	101.6 \pm 0.4	-0.8 \pm 0.8	-0.5 \pm 0.4

Table 4 (Continued)

Location Nr (#)	Grass pMC ($\pm 1s$)	Tree leaf pMC ($\pm 1s$)	Grass Fossil C ratio (%)	Tree leaf Fossil C ratio (%)
<i>Great Forest Debrecen</i>				
34	100.5 \pm 0.4	100.7 \pm 0.4	0.5 \pm 0.6	0.4 \pm 0.6
35	101.4 \pm 0.4	—	-0.3 \pm 0.6	—
Average	100.9 \pm 0.6		0.1 \pm 0.6	
Mean average	98.8 \pm 2.4	100.2 \pm 1.2	2.5 \pm 2.5	0.9 \pm 1.2

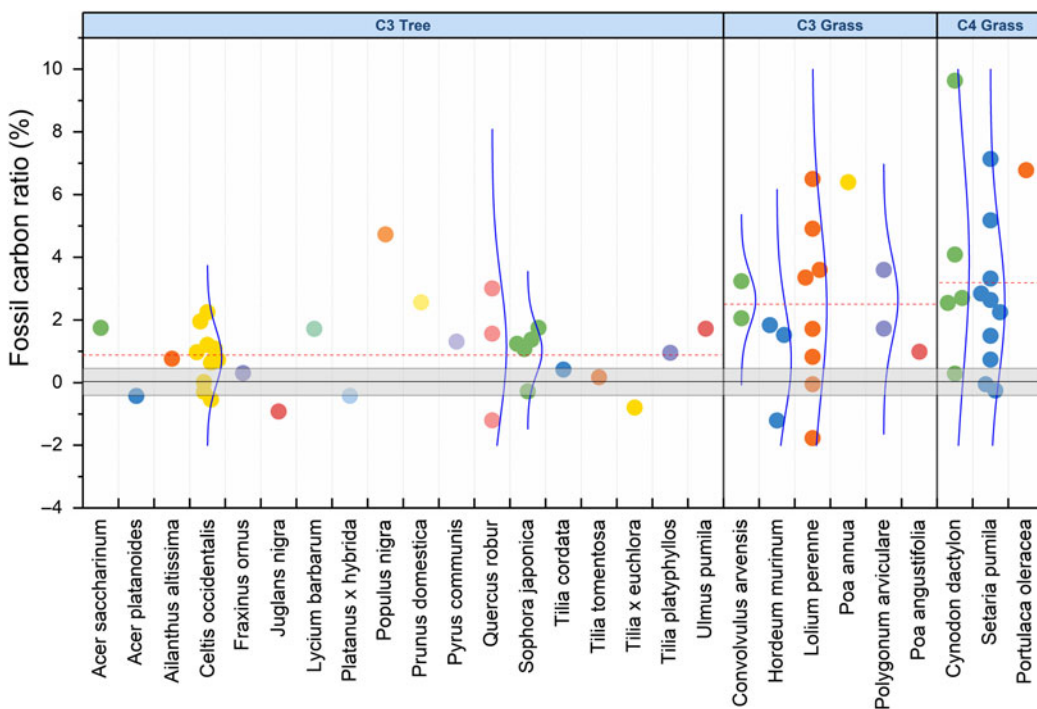


Figure 2 Fossil carbon content of different species and photosynthetic pathway. Solid blue curves are the histogram of the fossil carbon content of different species, dashed lines are the mean fossil carbon ratio of different photosynthesis pathway groups, the grey band around 0 % fossil carbon content is the error of the measurement.

in forested areas, where the soil biological activity and litter decomposition can contribute to an enriched ^{14}C signal (Trumbore 2000) or essentially no fossil carbon content. We suggest this is the case for sampling points no. 15 and 17, where the fossil carbon content in tree leaves is $-1.2 \pm 0.5\%$ and $-0.9 \pm 0.5\%$ in our study. The most ^{14}C depleted area is not in the downtown, thanks to the many pedestrian streets and limited traffic in the center of Debrecen city. The average fossil carbon content in the downtown is only 1.0 ± 1.0 and $0.4 \pm 0.8\%$ in the grass and tree leaf samples, respectively. The samples collected by busy crossroads and at the edge of the central area show the highest fossil carbon ratio, where the average fossil carbon

Table 5 Samples at the backyard of Atomki.

Sampling point	pMC of the grass \pm pMC	pMC of the tree \pm pMC	Fossil carbon ratio in grass % \pm %	Fossil carbon ratio in tree % \pm %
A	101.0 \pm 0.4	101.8 \pm 0.4	0.1 \pm 0.6	-0.7 \pm 0.6
B	99.9 \pm 0.4	—	1.1 \pm 0.6	—
C	—	102.3 \pm 0.5	—	-1.2 \pm 0.6
D	99.1 \pm 0.4	—	2.0 \pm 0.6	—
E	100.9 \pm 0.4	100.7 \pm 0.4	0.2 \pm 0.6	0.3 \pm 0.6
F	101.9 \pm 0.4	102.3 \pm 0.4	-0.9 \pm 0.6	-1.2 \pm 0.6
G	100.8 \pm 0.4	101.0 \pm 0.4	0.3 \pm 0.6	0.1 \pm 0.6
H	99.9 \pm 0.4	101.5 \pm 0.4	1.1 \pm 0.6	-0.4 \pm 0.6
Average	100.5 \pm 0.9	101.6 \pm 0.7	0.6 \pm 0.9	-0.5 \pm 0.6

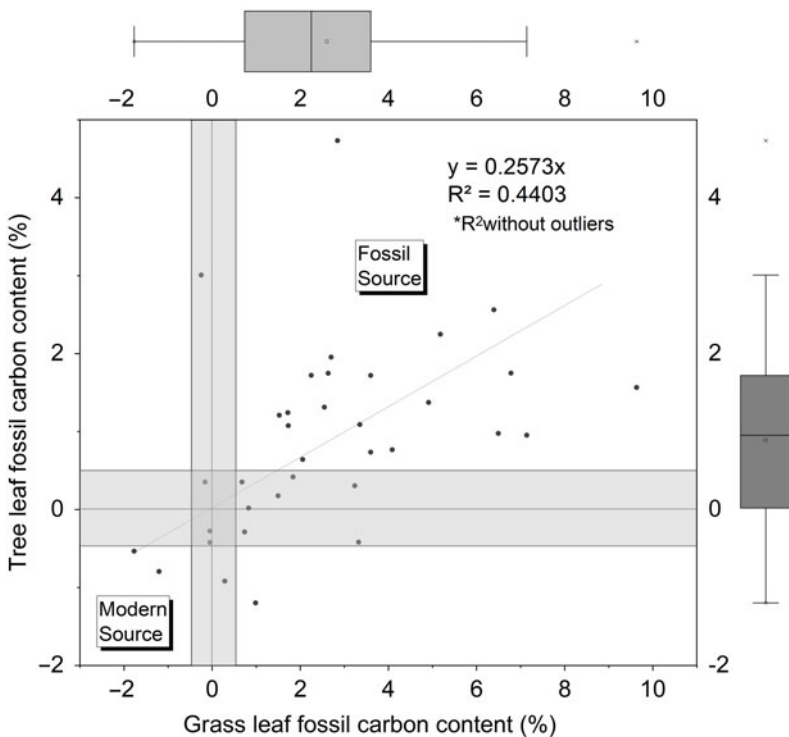


Figure 3 Correlation between the fossil carbon ratio of tree and grass leaf sample pairs. The grey bar represents the uncertainty the AMS measurement and fossil carbon content calculation. The box-plot chart represents distribution of these data.

content in the grass samples is $3.8 \pm 2.4\%$, and the highest fossil contribution was $9.6 \pm 0.7\%$ in a crossroad at the edge of the downtown, at sampling point no. 5. For these areas, the fossil contribution in five cases of 21 grass samples exceeded 5%, and the value was higher than 2% in four cases. The average fossil contributions in tree leaves at the busy crossroads and the edge of the downtown were $1.5 \pm 1.3\%$ and $1.3 \pm 0.5\%$, respectively.

In other districts, there are some outlier samples that can be explained by local conditions. The tree leaf sample no. 12 in the botanical garden has a higher fossil carbon content of $3.0 \pm 0.5\%$. This sampling point is located in the botanical garden of the University of Debrecen, far from busy crossroads, but close to the power plant of the Clinical Center of Debrecen, see [Figure 1](#). The situation for sampling point no. 28 is complex, because it is located by a busy crossroads and also close to the Debrecen electrical power plant. The fossil carbon content is higher in the tree leaf sample ($4.7 \pm 0.7\%$) than in the grass ($2.7 \pm 0.6\%$). In these two cases (sampling points 12 and 28), the atmospheric CO₂ emissions of the power plants are high enough to increase fossil carbon content of nearby tree leaves to similar levels as in the vicinity of busy crossroads. Besides the sources discussed, many other factors can influence the fossil carbon content of the local atmospheric CO₂ such as the design of the city. As the [Figure 1](#) and [Table 4](#) shows, densely populated areas have higher fossil carbon content. Traffic jams occur more frequently at these areas, which result in more concentrated fossil CO₂ emission. Moreover, high residential buildings and long block of flats can create a local barrier to mixing and refreshing of the air, by blocking the path of prevailing winds. Around these densely populated areas where the local and transit traffic also high, such as in the case of the 5,7,8,10,11,21 sampling points, these properties can amplify each other and create good conditions for the ¹⁴C depletion by the increased fossil CO₂ emissions from traffic ([Figure 1](#)).

CONCLUSION

Eighty-two plant samples from 36 different locations were measured in the region of Debrecen, Hungary. In our study, the fossil load of plants deriving from different type of urban areas, such as downtown, suburban areas and forests were investigated. The base reference level for fossil carbon load calculations given by the local atmospheric ¹⁴CO₂ information. The results from the courtyard of HEKAL show there is no clear difference compared to the ¹⁴CO₂ results of the local sampling station located here, consequently there is no significant fossil carbon contribution in this area during the vegetation period. Fossil carbon ratios were calculated for all samples and show a wide range of fossil and modern carbon load (from -1.9% to 9.6%). It is a narrower range in the case of tree leaves alone around a relatively low average fossil carbon load ($0.9 \pm 1.2\%$, $n = 35$). However in grass leaf samples, the average fossil carbon content is $2.5 \pm 2.5\%$ ($n = 35$). Our data show a relatively strong correlation between the grass leaf-tree leaf sample pairs and suggest that the tree leaves have just about 25% of fossil carbon content compared to their corresponding grass-sample pairs, in average. This might be an indication of how rapidly the traffic induced CO₂ emission can be diluted as a function of distance from the road. There are observable and higher fossil carbon load in local scale at the busy crossroads, as high as $9.6 \pm 0.7\%$ at ground level and $4.7 \pm 0.7\%$ at the height of tree leaves. In contrast, there is a clearly visible modern, post-bomb carbon emission from wood burning or soil CO₂ emission and litter decomposition in the suburbs, which can result in an apparently small negative fossil carbon load. Our study shows that the deciduous tree and grass samples can easily be applied for monitoring the ¹⁴C level and fossil carbon load. This approach could be a reliable and relatively cheap method to monitor the local atmospheric ¹⁴C level in CO₂ not just for close to nuclear facilities, but the vicinity of fossil loaded areas. Our results highlight the importance of collecting samples from the local vegetation as a record of local fossil-fuel and modern-carbon contributions to the CO₂ load.

ACKNOWLEDGMENTS

The research was supported by the European Union and the State of Hungary, co-financed by the European Regional Development Fund in the project of GINOP-2.3.2-15-2016-00009 “ICER.”

REFERENCES

- Alessio M, Anselmi S, Conforto L, Improta S, Manes F, Manfra L. 2002. Radiocarbon as a biomarker of urban pollution in leaves of evergreen species sampled in Rome and in rural areas (Lazio-Central Italy). *Atmospheric Environment* 36:5405–5416.
- Baydoun R, Samad OEL, Nsouli B, Younes G. 2015. Measurement of ^{14}C content in leaves near a cement factory in Mount Lebanon. *Radiocarbon* 57:153–159.
- Buzinny M. 2006. Radioactive graphite dispersion in the environment in the vicinity of the Chernobyl Nuclear Power Plant. *Radiocarbon* 48(3): 451–458.
- Capano M, Marzaioli F, Sirignano C, Altieri S, Lubritto C, D’Onofrio A, Terrasi F. 2010. ^{14}C AMS measurements in three rings to estimate local fossil CO_2 in Bosco Fontana forest (Mantova, Italy). *Nuclear Instruments and Methods in Physics Research B* 268:1113–1116.
- Cook AC, Hainsworth LJ, Sorey ML, Evans WC, Southon JR. 2001. Radiocarbon studies of plant leaves and tree rings from Mammoth Mountain, CA: a long-term record of magmatic CO_2 release. *Chemical Geology* 177:117–131.
- Druffel ERM, Griffin S. 1995. Radiocarbon in the tropospheric CO_2 and organic materials from selected Northern Hemisphere sites. *Radiocarbon* 37(3):883–888.
- Graven HD. 2015. Impact of fossil fuel emissions on atmospheric radiocarbon and various applications of radiocarbon over this century. *Proceedings of the National Academy of Sciences of the United States of America* 112(31):9542–9545.
- Haszpra L, Barcza Z, Davis KJ, Tarcay K. 2005. Long-term tall tower carbon dioxide flux monitoring over an area of mixed vegetation, *Agricultural and Forest Meteorology* 132:58–77.
- Heal MR, Naysmith P, Cook GT, Xu S, Duran TR, Harrison RM. 2011. Application of ^{14}C analyses to source apportionment of carbonaceous $\text{PM}_{2.5}$ in the UK. *Atmospheric Environment* 45: 2341–2348.
- Hsueh DY, Krakauer NY, Randerson JT, Xu X, Trumbore SE, Southon JR. 2007. Regional patterns of radiocarbon and fossil fuel-derived CO_2 in surface air across North America. *Geophysical Research Letters* 34:L02816
- Janovics R, Futó I, Molnár M. 2018. Sealed tube combustion method with MnO_2 for AMS ^{14}C measurement. *Radiocarbon* 60(5):1347–1355.
- Janovics R, Kern Z, Güttler D, Wacker L, Barnabás I, Molnár M. 2013. Radiocarbon impact on a nearby tree of a light-water VVER-type nuclear power plant, Paks, Hungary. *Radiocarbon* 55(2–3):826–832.
- Király G, editor. 2009. Új magyar fűvészkönyv. Magyarország hajtásos növényei. Határozókulcsok. New Hungarian Herbal. The Vascular Plants of Hungary. Identification key. Aggtelek National Park Directorate, Jószaafő: 616
- Kuc T. 1986. Carbon isotopes in atmospheric CO_2 of the Krakow region: a two-year record. *Radiocarbon* 28(2A):649–657.
- Levin I, Kromer B, Hammer S. 2013. Atmospheric $\Delta^{14}\text{CO}_2$ trend in Western European background air from 2000 to 2012. *Tellus B* 65(1):20092.
- Levin I, Kromer B, Schoch-Fischer H, Bruns M, Münnich M, Berdau D, Vogel JC, Münnich K. 1985. 25 years of tropospheric ^{14}C observations in central Europe. *Radiocarbon* 27(1):1–19.
- Levin I, Hesshaimer V. 2000. Radiocarbon—a unique tracer of global carbon cycle dynamics. *Radiocarbon* 42(1):69–80.
- Major I, Furu E, Haszpra L, Kertész Zs, Molnár M. 2015. One-year-long continuous and synchronous data set of fossil carbon in atmospheric $\text{PM}_{2.5}$ and carbon dioxide in Debrecen, Hungary. *Radiocarbon* 57(5):991–1002.
- Major I, Haszpra L, Rinyu L, Futó I, Bihari Á, Hammer S, Molnár M. 2018. Temporal variation of atmospheric fossil and modern CO_2 excess at a Central European rural tower station between 2008 and 2014. *Radiocarbon* 60(5):1285–1299.
- Molnár M, Bujtás T, Svingor É, Futó I, Svetlík I. 2007. Monitoring of atmospheric excess ^{14}C around Paks Nuclear Power Plant, Hungary. *Radiocarbon* 49(2):1031–1043.
- Molnár M, Haszpra L, Svingor É, Major I, Svetlík I. 2010a. Atmospheric fossil fuel CO_2 measurement using a field unit in a Central European city during the winter of 2008/09. *Radiocarbon* 52(2–3):835–845.
- Molnár M, Janovics R, Major I, Orsovski J, Gönczi R, Veres M, Leonard AG, Castle SM, Lange TE, Wacker L, Hajdas I, Jull AJT. 2013. Status report of the new AMS ^{14}C sample preparation lab of the Hertelendi Laboratory of Environmental Studies (Debrecen, Hungary). *Radiocarbon* 55(2–3):665–676.
- Molnár M, Major I, Haszpra L, Svetlík I, Svingor É, Veres M. 2010b. Fossil fuel CO_2 estimation by

- atmospheric ^{14}C measurement and CO_2 mixing ratios in the city of Debrecen, Hungary. *Journal of Radioanalytical and Nuclear Chemistry* 286(2):471–476.
- Molnár VÉ, Tóthmérész B, Szabó S, Simon E. 2018. Urban tree leaves' chlorophyll-a content as a proxy of urbanization. *Air Quality, Atmosphere & Health* 11(6):665–671.
- Ndeye M, Sène M, Diop D, Saliège J-F. 2017. Anthropogenic CO_2 in the Dakar (Senegal) urban area deduced from ^{14}C concentration in tree leaves. *Radiocarbon* 59(3):1009–1019.
- Nydal R, Lövseth K. 1983. Tracing bomb ^{14}C in the atmosphere 1962–1980. *Journal of Geophysical Research* 88(6):3621–3642.
- OKIR. 2017. Országos Környezetvédelmi Információs Rendszer/National Environmental Information System, Hungary. Available at: <http://web.okir.hu/sse/?group=PRTR>.
- Park JH, Hong W, Xu X, Park G, Sung KS, Sung K, Lee JG, Nakanishi T, Park H-S. 2015. The distribution of $\Delta^{14}\text{C}$ in Korea from 2010 to 2013. *Nuclear Instruments and Methods in Physics Research B* 361:609–613.
- Pawelczyk S, Pazdur A. 2004. Carbon isotopic composition of tree rings as a tool for biomonitoring CO_2 level. *Radiocarbon* 46(2):701–719.
- Quarta G, Rizzo GA, D'elia M, Calcagnile L. 2007. Spatial and temporal reconstruction of the dispersion of anthropogenic fossil CO_2 by ^{14}C AMS measurements of plant material. *Nuclear Instruments and Methods in Physics Research B* 259:421–425.
- Rakowski AZ. 2011. Radiocarbon method in monitoring of fossil fuel emission. *Geochronometria* 38(4):314–324.
- Riley WJ, Hsueh DY, Randerson JT, Fischer ML, Hatch ML, Pataki DE, Wang W, Goulden ML. 2008. Where do fossil fuel carbon dioxide emissions from California go? An analysis based on radiocarbon observations and an atmospheric transport model. *Journal of Geophysical Research* 113(G4):G04002.
- Rinyu L, Molnár M, Major I, Nagy T, Veres M, Kimák Á, Wacker L, Synal H-A. 2013. Optimization of sealed tube graphitization method for environmental ^{14}C studies using MICADAS. *Nuclear Instruments and Methods in Physics Research B* 294:270–275.
- Shore JS, Cook GT. 1995. The ^{14}C content of modern vegetation samples from the flanks of the Katla volcano, Southern Iceland. *Radiocarbon* 37(2):525–529.
- Simon E, Baranyai E, Braun M, Cserháti C, Fábrián I, Tóthmérész B. 2014. Elemental concentrations in deposited dust on leaves along an urbanization gradient. *Science of the Total Environment* 490:514–520.
- Southon JR, Magana AL. 2010. A comparison of cellulose extraction and ABA pretreatment methods for AMS ^{14}C dating of ancient wood. *Radiocarbon* 52(2–3):1371–1379.
- Stenström KE, Skog G, Georgiadou E, Grenberg J, Johansson A. 2011. A guide to radiocarbon units and calculations: Lund University [Sweden], Department of Physics, Division of Nuclear Physics Internal Report LUNFD6(NFFR-3111)/1-17(2011).
- Suess HE. 1955. Radiocarbon concentration in modern wood. *Science* 122:415–417.
- Trumbore S. 2000. Age of soil organic matter and soil respiration: radiocarbon constraints on belowground C dynamics. *Ecological Applications* 10(2):399–411.
- Varga T, Major I, Janovics R, Kurucz J, Veres M, Jull AJT, Péter M, Molnár M. 2018. High-precision biogenic fraction analyses of liquid fuels by ^{14}C AMS at HEKAL. *Radiocarbon* 60(5):1317–1325.
- Veres M, Hertelendi E, Uchrin Gy, Csaba E, Barnabás I, Ormai P, Volent G, Futó I. 1995. Concentration of radiocarbon and its chemical forms in gaseous effluents, environmental air, nuclear waste and primary water of a pressurized water reactor power plant in Hungary. *Radiocarbon* 37(2):497–504.
- Xi XT, Ding XF, Fu DP, Zhou LP, Liu KX. 2013. $\Delta^{14}\text{C}$ level of annual plants and fossil derived CO_2 distribution across different regions of China. *Nuclear Instruments and Methods in Physics Research B* 294:515–519.
- Zhou W, Wu S, Huo W, Xiong X, Cheng P, Lu X, Niu Z. 2014. Tracing fossil fuel CO_2 using $\Delta^{14}\text{C}$ in Xi'an City, China. *Atmospheric Environment* 94:538–545.